CIM

Technical Paper

Blasting

A numerical description of the formation of a crater in rock blasting

L. Liu, Prime Perforating Systems Ltd., Calgary, Alberta, and

P.D. Katsabanis, Department of Mining Engineering, Queen's University, Kingston, Ontario

KEYWORDS: Blasting, Rock fragmentation mechanisms, Simulations.

Paper reviewed and approved for publication by the Metal Mining Division of CIM.

ABSTRACT

A newly developed damage model was used in the study of rock fragmentation mechanisms involved in crater blasting. Simulations show that at the detonation of the explosive charge, a crushed zone around the explosive charge is formed due to compressive failure and then a strong pressure wave is sent out forming a pressurized ring that propagates at the dilatation wave velocity. As the pressurized ring leaves the crushed zone, two tensile stress components perpendicular to the radial stress are developed in response to the action of the radial pressure, causing tensile failure and forming a damage zone around the charge. The formation of this damage zone is quite independent of the depth of the explosive charge provided there is no interference by the reflection from the free face. When the pressurized ring reaches the free face, it is reflected there and causes rock failure on the ground surface that forms another damage zone. Under the simulation conditions, it is revealed that the depth of charge is a factor controlling the relationship between the two damage zones. At a depth smaller than the optimum, the two damage zones coalesce into one and there is excessive rock breakage; otherwise, the two damage zones tend to isolate from each other with the increase in the depth of charge. Calculations of fragmentation indicate that the average fragment size increases and the uniformity of fragments decreases when the depth of charge increases as observed in practical blasting.

Introduction

Rock blasting with the borehole perpendicular to an only free face is normally termed crater blasting. It has undergone extensive studies during the last few decades because of its importance in theory, as a window to view the fundamental mechanisms of explosively loaded rock fragmentation and in practical applications. Despite the efforts so far, some aspects of the physical processes involved in crater blasting still remain to be unveiled. The present work represents a new effort to explore such mechanisms, aimed at understanding the physical processes involved in crater blasting, and assisting practical blasting operations and improving production efficiency.

In cratering studies, it has long been a controversial topic as to whether the explosion gas or the stress wave plays a more important role in the formation of a crater. The most influential cratering theory may be Livingston's spherical charge cratering theory (Livingston, 1962; Lang, 1976; Lang et al., 1977; Bauer et al., 1965) which is an empirical one. Livingston's theory believes in gas pressure domination and it assumes that the pressure applied to the rock mass by the explosion gas is responsible for rock failure. However, since the time of Livingston, numerous cratering studies have been published and seem to prove that the rock breaking process is dominated by the stress wave generated by the detonation of the explosive charge.

The tests conducted by Duvall and Atchison (1957) show that the stress wave in the rock transmits energy to the free face, which is reflected and causes significant rock breakage without the penetration of the explosion gas or the direct effects of explosion gas pressure. Simha et al. (1987) and Hommert et al. (1987) investigated the usefulness of stemming in rock blasting, and they reported that even when blasting with unstemmed boreholes, little difference was observed in the craters formed, and stress waves appear to be much more important in the cratering process. Brinkman (1987) found that shock energy that is transmitted into the rock mass by shock/stress waves appears to be most effective in fracturing near the blasthole where maximum loading occurs.

Research work by a number of investigators further suggests that the fracture network is formed synchronously with material failure. According to Brinkman (1987), fragment sizes are controlled primarily by the stress waves. Zhao et al. (1993) conducted experiments to observe the formation of fragment patterns in rock specimens. They reported that the fractal dimension (a variable used to describe fragment size distribution) increased with stress level in

Liqing Liu obtained his B.Sc. (1983) and M.Sc. (1986) degrees from the Department of Mining Engineering, Central South University of Technology (CSUT), Changsha, China. From 1986 to 1992, he worked as a mining engineer in Beijing General Research Institute of Mining and Metallurgy (BGRIMM) where he was involved in the development of China's electro magnetic induction initiation systems and of underground large-diameter hole mining methods. He continued his education by joining Queen's University in 1992 where he explored some fundamental problems in rock blasting, including the damage process, cratering theory, air-decking/decoupling and blasting with accurate timing. He received his Ph.D. at the end of 1996 for his research and studies. Upon his graduation from Queen's, Dr. Liu joined Canada's oil industry and is currently a research and development engineer at Prime Perforating Systems Ltd. in Calgary, Alberta.
Dr. Liu's research interests include the development of initiation devices and other explosive products for oil well applications and mining engineering, numerical modelling of rock blasting and perforation, etc. He is a member of the Canadian Institute of Mining, Metallurgy and Petroleum (CIM) and International Society of Explosives Engineers (SEE).

P.D. Katsabanis, associate professor in mining engineering, Queen's Univsersity, received his B.Sc. from the National Technical University of Athens in mining and metallurgical engineering and obtained his M.Sc. (Eng.) and Ph.D. degrees from Queen's University. His research activities include the investigation of sulphide and other reactive dusts explosions, the numerical modelling of the sensitivity and performance of condensed explosives, the numerical modelling of the initiation of low density explosives, the determination of the equations of state for ideal and non-ideal explosives, the measurement of heat of high explosives using detonation calorimetry, the experimental determination of detonation parameters in boreholes, the optimization of explosive compositions, the study of sympthetic detonations and shock and static pressure desensitization of explosives, the numerical modelling of fragmentation, the experimental determination of detonator accuracy and the optimization of blasting by using high speed photography.
Dr. Katsabanis is a member of the Canadian Institute of Mining, Metallurgy and Petroleum (CIM) and International Society of Explosives Engineers (SEE).

the stage of micro crack initiation and coalescence, but remained unchanged in the stage of macro crack development. After the crack pattern is formed, the stresses induced from the gas remaining in the borehole and gas penetrating into the near-borehole fracture network (late gas pressure effects) tend to drive cracks formed in the earlier stages of breakage rather than to create new fractures (Wilson, 1987).

In the aforementioned studies and in the present paper, all the rock materials investigated are brittle and hard rock as most commonly encountered in mining practice. It is assumed that the damage process, as well as the fragment formation in such rock types, can be reasonably modelled with a wave code.

The Methodology and Numerical Tool of Study

A continuum damage model developed by the authors (Liu and Katsabanis, 1997) was used in the present study. In this model, it is assumed that the pre-existing micro cracks in the rock mass are activated and grow in number when the volumetric tensile strain is larger than a critical value. The degradation of the material's stiffness resulting from the growth of micro cracks is measured by the probability of fracture, which is obtained by integrating a crack density function over time. The minimum damage value is 0.632, meaning that in order to form fragments, the micro cracks begin to coalesce with each other at this value. Fragment size is calculated considering the equilibrium between kinetic energy and fracture surface energy, with the changes in loading rate, stiffness and material density taken into account. The model was coded as user routines for the finite element program ABAQUS/Explicit (version 5.4, Hibbitt, Karlsson & Sorensson, 1994a). Simulation results obtained with the model satisfactorily reproduced actual blasting results (Liu, 1996).

Fig. 1. Finite element mesh of the geometrical model used in the numerical example.

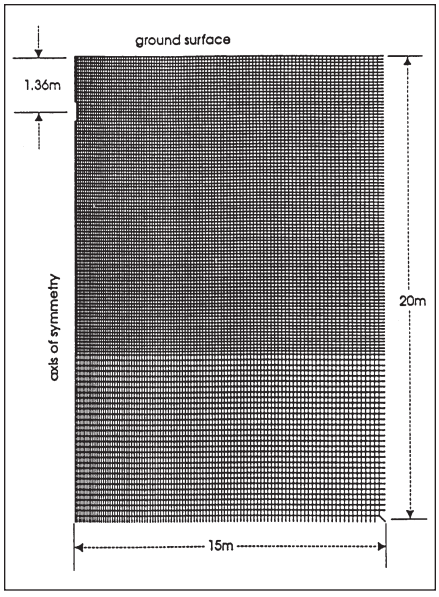

Table 1. Parameters of granite modelled

E,(GP)	n	Υ,(t/m^3)	σ_t,(MP)	a,(x10^{10})	β	u_c,(x10^{-3})	K_{IC}, (N/M$^{2/3}$,x10^6)
51.8	0.33	2.55	215	7	2	0.1411	3.1

Table 2. JWL equation of state parameters of emulsion used

A,(GPa)	B,(GPa)	R_1	R_2	v	E_0 ,(J/Kg,x10^6)	VOD, (m/s)	Υ_0,(g/cm^3)
214.36	0.182	4.2	0.9	0.15	3.2	5500	1.31

In the present work, crater blasting in an axisymmetric environment is simulated, i.e., the borehole is drilled perpendicular to an only free face (the ground surface). To trace the physical processes involved in the time interval from the initiation of the explosive charge to the final formation of a crater, a specific numerical example is used. In this example, it is assumed that the explosive used is an emulsion and the rock material modelled is the granite of the test site of Queen's University. This ensures that the simulation results have a basis of comparison with a series of practical cratering shots conducted in this laboratory (Rocque, 1992; Bawden et al., 1993; Katsabanis, 1994). The properties of the rock mass are listed in Table 1 and the JWL (Jones-Wilkins-Lee) equation of state parameters for emulsion are shown in Table 2. It is further assumed that the explosive charge is a small cylindrical column 480 mm in height, 90 mm in diameter, with a weight of 4 kg. The explosive column has a length/diameter ratio of 5.33 and it is initiated at its bottom.

The geometrical model is discretized as shown in Figure 1. The explosive charge is in the place of the opening to the left of the mesh. The depth of burial of the explosive charge refers to the distance from the gravity centre of the charge to the ground surface. The opening to the left of the mesh indicates the position of the explosive charge. The model has a geometry of 15 m by 20 m and it is bordered by infinite elements to simulate a non-reflective boundary with the purpose of reducing the total number of elements necessary in the model (Hibbitt, Karlsson & Sorensen Inc., 1994a). Only one section of the model is discretized taking advantage of its axisymmetry.

After a simulation, the variables of interest, such as stress, damage, etc., are assessed by reviewing their time histories. The overall simulated blasting results are assessed according to the total volume of fragments predicted, the diggability of the damage zones and the statistical fragment size distribution.

Formation of the Crushed Zone

During the detonation process, a high pressure from the explosive charge is applied to the rock mass. In this study, an elasto-plastic material model with kinematic hardening is used to describe the rock mass response under high pressure. It is assumed that if the yield stress is exceeded, plasticity occurs in the increment. The detailed algorithm of the material model under high pressure can be found in the user's manual of ABAQUS/Explicit (Hibbitt, Karlsson & Sorensen Inc., 1994b).

The reaction time of the explosive column of the study is 87.3 µs, based on an average detonation velocity of 5500 m/s. The pressure in the borehole wall is much higher than the compressive strength of the rock material (uniaxial compressive strength, 215 MPa for granite under study). At the time of 50 µs after initiation, the highest pressure in the borehole wall is 1280 MPa, while at 100 µs, it is 1490 MPa. Failed material points under such a high pressure form a thin layer in the borehole wall, generally called the crushed zone. At about 150 µs after initiation, the crushed zone has already been formed, while there is little change afterward. In the material model, compressive failure of a material point is represented by the equivalent plastic strain caused by pressure. The crushed zone surrounding the explosive chamber in the rock mass at 150 µs and 600 µs is represented by the equivalent plastic strain (SDV7) contours shown in Figures 2a and 2b. The thickness of the crushed zone at 150 µs that has an equivalent plastic strain larger than 4% is less than 100 mm. There is no obvious change in the thickness from 150 µs to 600 µs, although there is noticeable increase in the equivalent plastic strain value. Figure 3 shows the pressure contours along the whole model at 600 µs. It is shown that pressure higher than the UCS (uniaxial compressive strength) of granite (215 MPa) appears only in the region of the crushed zone. This is consistent with the experimental findings by Hakalehto (1969), who discovered that the maximum dynamic stress carrying capacity of a sandstone and a granite sample was approximately equal to the UCS. According to Comeau (1995), despite the very high pressure in the blasthole, rock material has a maximum stress transmission capacity which limits the value of the stress wave generated at or near the borehole. Excessive stress was mainly consumed by local damage at the input end. In the numerical example, it is consumed in the formation of the crushed zone. Although a significant amount of explosive energy is consumed in the formation of the crushed zone, the total volume of rock material damaged by compressive failure is negligible in practical blasting operations.

Fig. 2. Formation of the crushed zone (contours of the equivalent plastic strain): (a) at 150 μs after initiation; (b) at 600 μs after initiation.

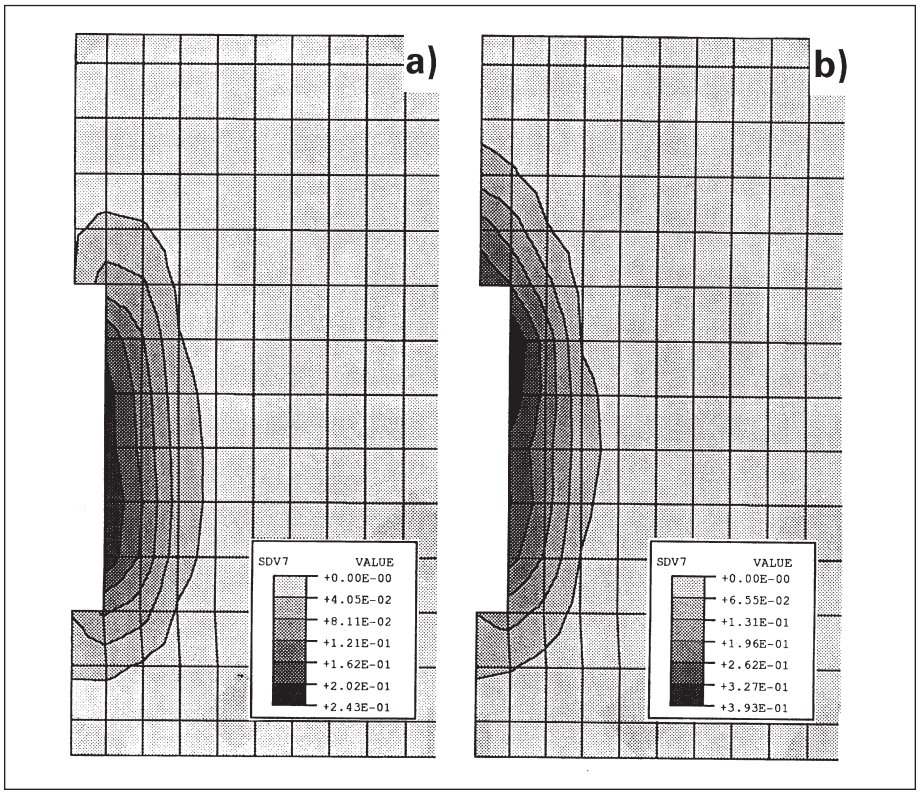

Fig. 3. Pressure contours in the vicinity of the explosive chamber at 600 μs after initiation, showing the high pressure in the borehole is mainly equilibrated by the crushed zone. Pressure unit in Pa.

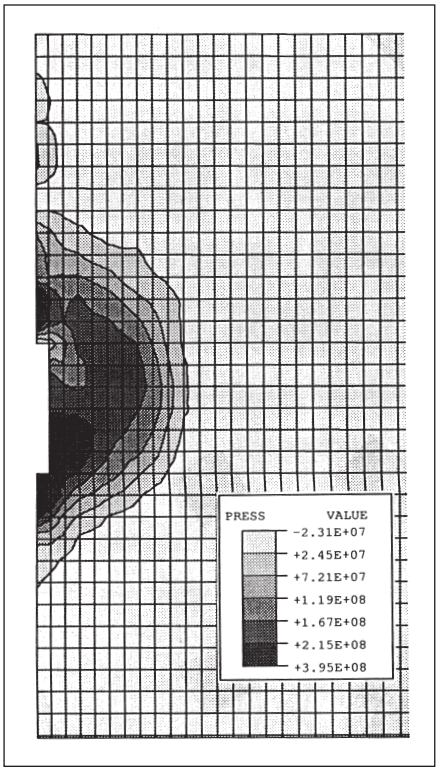

Fig. 4. An illustration of the concept of a pressurized ring. A pressurized ring generated by 4 kg emulsion, 200 μs after initiation. Pressure unit in Pa.

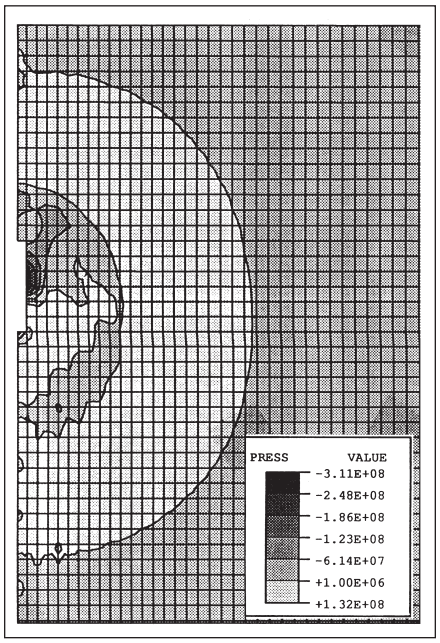

Formation of the Lower Damage Zone

When an explosive charge is buried at a large depth, experimental observations show that a small crater is formed by slabbing on the ground surface, and the larger the depth of burial, the smaller the surface crater. However, in addition to the damage zone on the ground surface, there exists another damage zone immediately surrounding the explosive charge. In this paper, the damage zone on the ground surface is called the upper damage zone and the one immdiately surrounding the explosive charge the lower damage zone. If the rock material between the two damage zones has undergone very little damage, the lower damage zone will be entirely entrapped below it and cannot be excavated. The existence and characteristics of the lower damage zone have been studied using modern instrumentation (Katsabanis, 1994; Bawden et al., 1993; LeBlanc et al., 1995).

Existence of a Pressurized Ring Prior to Tensile Failure

After the formation of the crushed zone, the pressure front travels outward and leaves the crushed zone behind it. It has been found that the pressure front at this stage does not cause any kind of material failure immediately. Instead, under the action of the pressure front, a layer of material is compressed elastically which forms a pressurized ring. The pressurized ring follows the pressure front at the same velocity as the latter (dilatation wave velocity). It will be shown that the pressurized ring is, in fact, responsible for the formation of the two damage zones by inducing tensile stresses or by reflection.

Figure 4 shows the pressurized ring formed in the rock mass 200 μs after initiation of the explosive charge. As the stress in the pressurized ring is in nature dominantly compressive but lower than the compressive strength of the rock material, neither tensile nor compressive failure will occur, i.e., rock material in the pressurized ring is only compressed elastically. However, the energy available for subsequent tensile failure and a lot of other information regarding the fracture process can be obtained through the analysis of the pressurized ring. The characteristics of the pressurized ring will be discussed later in this paper.

Tensile Failure behind the Pressurized Ring

The deformation of the pressurized ring is caused by the radial stress component. Because the deformation is elastic in nature, it does not cause any damage to the rock material. However, two tensile stress components emerge in response to the action of the radial compressive stress.

For a material point subjected to a radial stress σ_r, the hoop stress σ_u and the vertical stress σ_z are developed in response to the action of σ_r in order to achieve equilibrium. The histories of the three stress components for a selected element in the numerical example are shown in Figure 5. The element is at the same depth as the top of the explosive charge but 0.62 m away from the axis of symmetry. As shown in Figure 5, the radial compressive stress σ_r increases steadily in magnitude when the pressurized ring reaches this element at about

Fig. 5. Histories of three stress components: hoop stress σ_u, vertical stress σ_z and radial stress σ_r of a selected element.

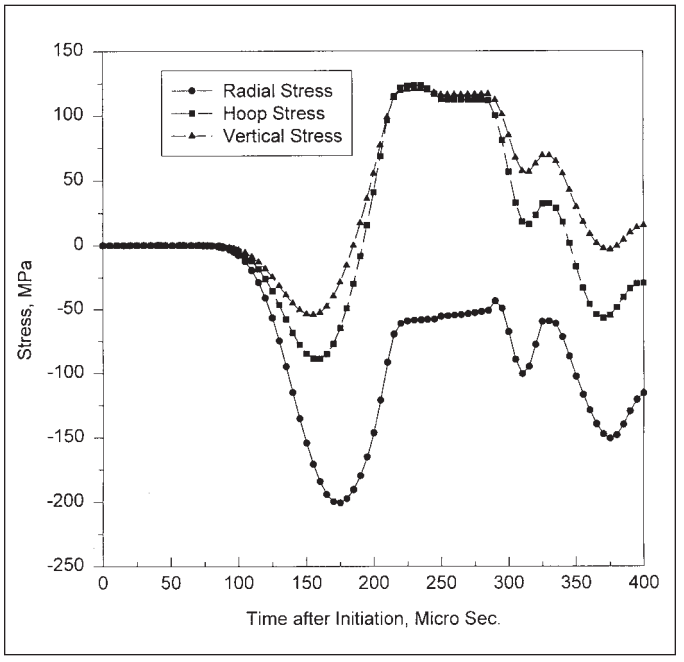

Fig. 6. Combined effect of three stress components and the damage growth history of the selected element.

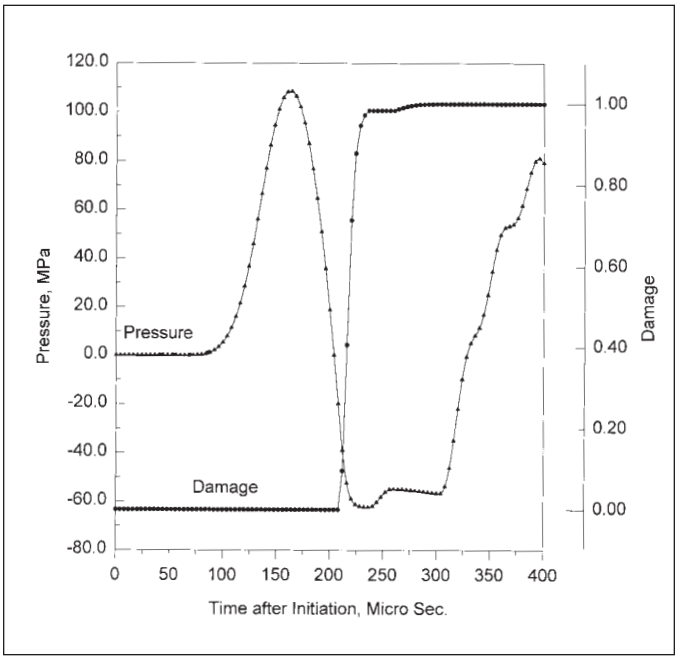

100 µs after initiation of the explosive charge. At the time the element is within the pressurized ring, the stress state is dominated by the compressive stress and the element is deformed (compressed) elastically while no damage takes place. The hoop stress σ_u and the vertical stress σ_z are shown briefly compressive upon the arrival of the pressurized ring because there is an incident angle between the radial stress of the pressurized ring and the radial direction of the coordinate system. The stresses are plotted in accordance with the latter. The pressurized ring travels through this element in about 100 µs, i.e., the duration this element remains being compressed is about 100 µs. Consequently, the frequency of the loading wave experienced by this element can be calculated to be 5 KHz. During this period, the element absorbs energy for later expansion and breakage. After the passage of the pressurized ring, two tensile stress components are developed and dominate the stress state in this element. At this point, the tensile stresses are much higher than the static tensile strength (approximately 18 MPa for granite), micro cracks in the element are activated and grow rapidly in number, causing permanent damage to the element. The combined effects of the three stress components on the damage process of the rock element are shown in Figure 6, where pressure is defined as the average value of the three stress components with the sign reversed according to the concept in continuum mechanics. As shown in Figure 6, the damage coefficient remains zero after initiation and while the element is being compressed. It is after 200 µs when the pressurized ring has passed the element and the tensile stress (negative pressure) begins to dominate, that the damage increases rapidly and steadily until full fragmentation (damage value = 1.0) of the rock element occurs.

This is how the lower damage zone is formed and the mechanism seems to agree with Kutter and Fairhurst (1971). According to their work, near borehole radial fracturing is initiated by tensile hoop stresses created in response to the compressive borehole stresses. As the pressurized ring travels forward, the radial stress and the resultant tangential stresses decay very rapidly. At a certain point, the tangential tensile stresses become too low to further induce tensile failure. Figure 7 shows the status of the pressurized ring and the lower damage zone formed at 300 µs after initiation (in Fig. 7b, SDV9 represents damage). Because the formation of this damage zone is driven by the outgoing pressure front, it is independent of the depth of burial of the explosive charge, provided there is no interference by reflection from the ground surface at small depths.

Formation of the Upper Damage Zone

After its formation, the pressurized ring propagates outward in all directions. The elastic energy contained in the parts that travel toward the infinite bottom and side boundaries is dissipated in the rock mass without contribution to rock fracture and fragmentation. Only the elastic energy contained in the part of the ring that travels toward the ground surface and is reflected there has the potential to further break the rock material creating the upper damage zone.

In the numerical example, the topmost part of the pressurized ring reaches the point where the borehole centre line meets the ground surface and the reflection of the compressional wave begins there, creating spalling. On the ground surface, the reflection of the pressurized ring expands rapidly from the borehole centre outward. At the later stage of the lower damage zone formation, the pressurized ring meets the ground surface at 300 µs after initiation and a part of it is being reflected and superposes with the unreflected part of the pressurized ring (Fig. 7a). Tensile stress due to reflection has not appeared yet at this time. The area below the part of the pressurized ring being reflected is shown tensile but the tensile stress is still the tensile tail of the pressurized ring as described in the previous section. As a result, there is still no damage caused by reflection, as demonstrated in Figure 7b. As the reflection wave expands outward from borehole centre, tensile stress due to reflection comes into play and causes rock failure near the ground surface. It is evident that the area having the highest tensile stress is near the borehole collar and below the ground surface. In the numerical example, on account of the small depth of charge, this area combines with the tensile tail of the pressurized ring. This combination is not always possible and depends on the depth of burial of the charge. When the depth of burial is large, separate damage zones are formed. Figure 8 shows the pressurized ring being reflected from the ground surface and the upper damage zone established on top of the lower damage zone at 400 µs after initiation. As shown in Figure 8a, the value of the tensile stress due to reflection is 26 MPa to 49MPa, which is much higher than the static tensile strength of

the rock material (approximately 18 MPa). Consequently, micro cracks are activated and tensile failure takes place in this area, resulting in the damage contours shown in Figure 8b. As the upper part of the pressurized ring travels further away from the borehole centre, reflection takes place behind it and below the ground surface, causing tensile damage to the rock material in its path. This process will continue until the reflection wave is too weak to create more damage. The upper damage zone is gradually established in this manner by the reflection of the pressurized ring from the ground surface. The final damage contour at 800 µs after initiation is shown in Figure 9. Due to the small depth of burial, the lower and upper damage zones have combined into one, forming a large crater that can be excavated.

Fig. 7. The status of the pressurized ring and the lower damage zone formed formed at 300 µs after initiation: (a) the pressurized ring, pressure unit in Pa; (b) the lower damage zone (damage represented by SDV9).

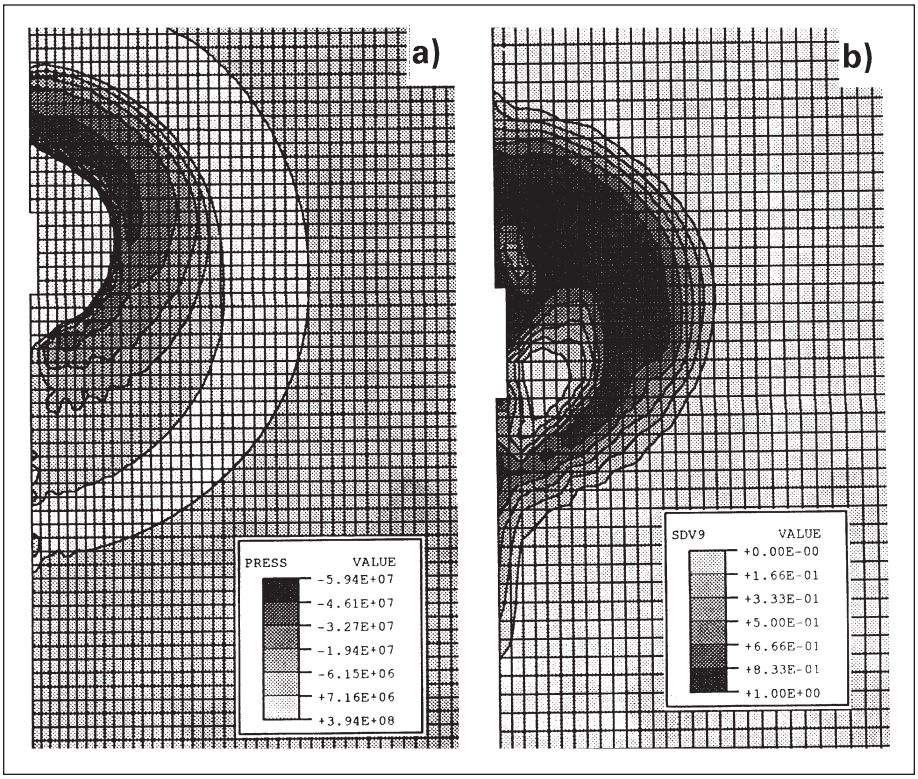

Fig. 8. Formation of the upper damage zone by the reflection of the pressurized ring from the ground surface: (a) pressurized ring at 400 µs, pressure unit in Pa; (b) damage at 400 µs.

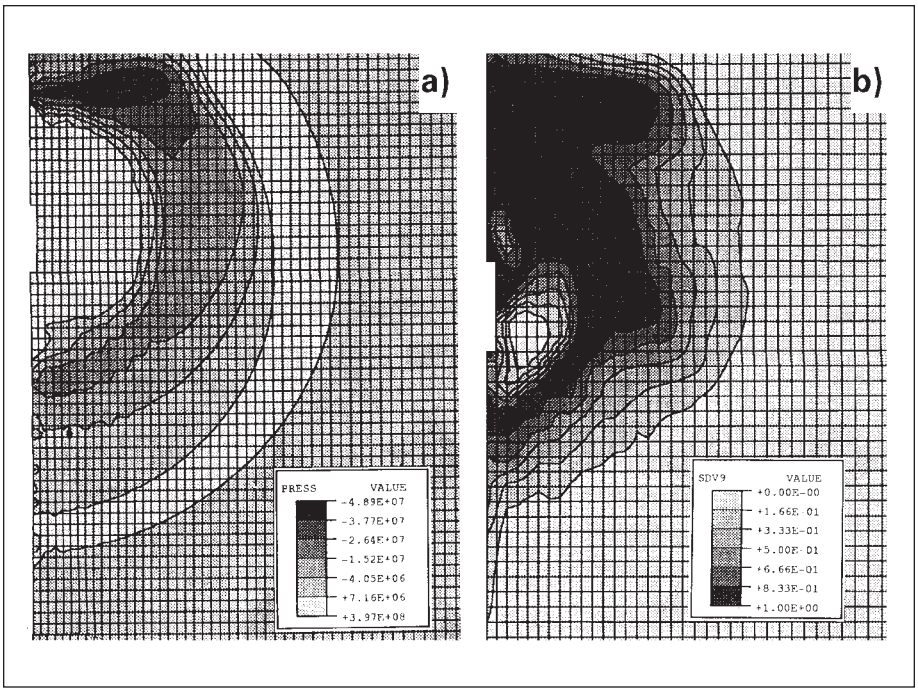

Influence of the Depth of Charge

As described previously, the formation of the lower damage zone is quite independent of the depth of charge. The depth of charge influences the final blasting results by influencing the formation of the upper damage zone, its relationship with the lower damage zone, its volume of fragments and the size distribution of the fragments.

Coalescence and Separation of Two Damage Zones

When the explosive charge is placed closer to the ground surface, the rock material in a small area above the top level of the explosive charge and below the ground surface may be over fractured during the formation of the lower damage zone and the subsequent upper damage zone. Because this area is within the range of influence of both damage zones, its existence makes the two damage zones interact with each other. However, a depth of burial that is too small tends to waste the energy in the reflection wave in fracturing the rock material that has already been fractured during the formation of the lower damage zone, causing excessive breakage. The total volume of fragments that can be excavated and the fragment size distribution are of primary concern in practical blasts and will be used to describe the influence of the depth of burial.

The simulated total volume of fragments as a function of the depth of burial is plotted in Figure 10. The total volume of fragments shown

Fig. 9. Final damage contours at 800 µs after initiation, showing both the lower and the upper damage zones formed and coalesced into one.

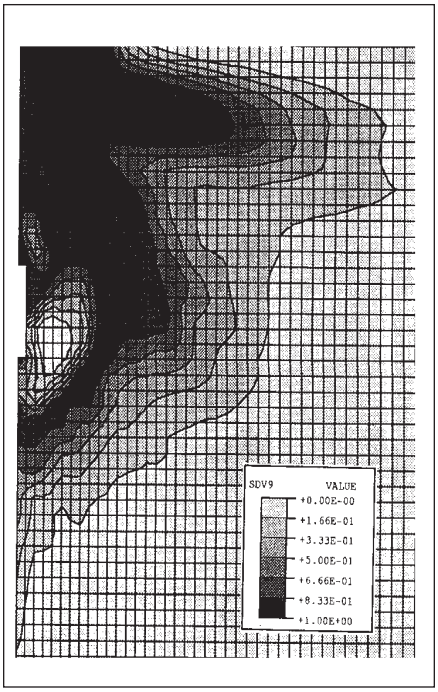

Fig. 10. Volume of fragments as a function of depth of burial.

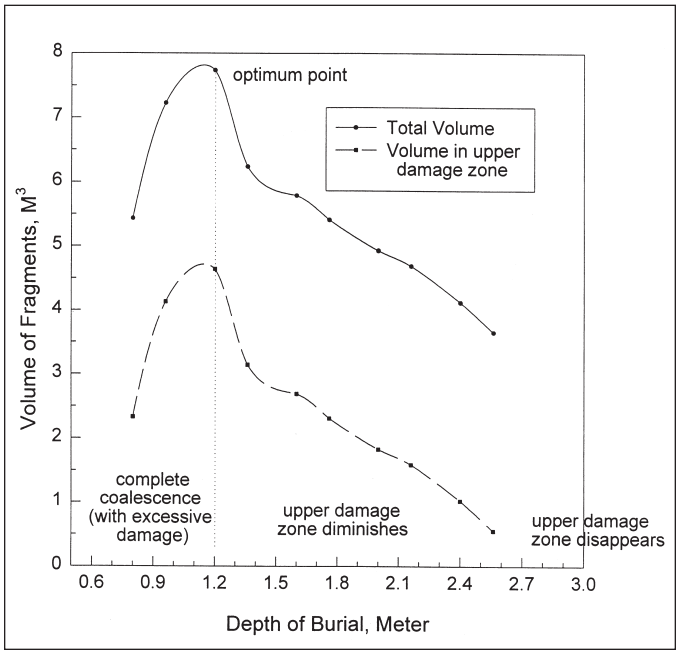

Fig. 12. Fragment size distribution at different depths of burial.

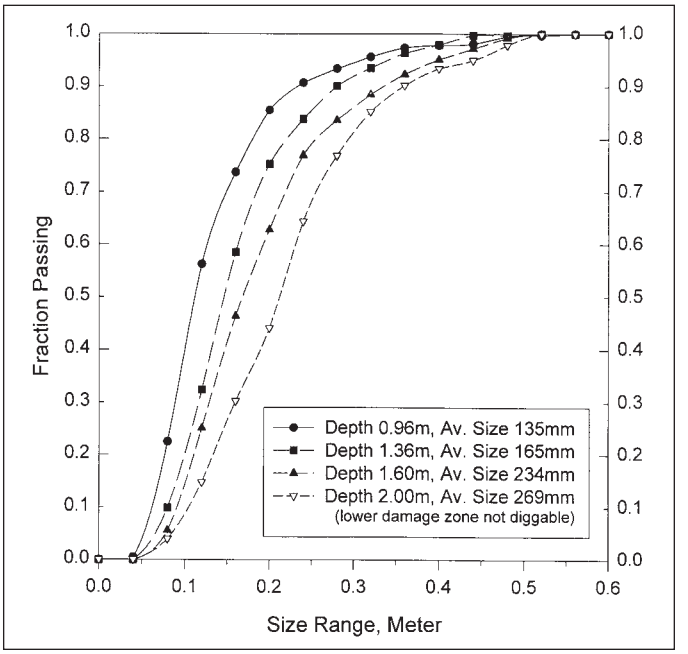

Fig. 11. Damage contours at a depth of burial of 2.56 m, showing the upper damage zone reduced in size and the two damage zones completely separated.

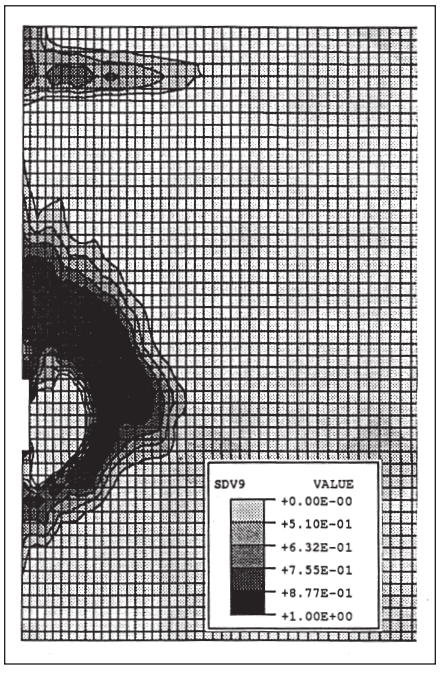

here is the sum of the volume of two damage zones, either coalesced or separated. The volume of the lower damage zone is 3.10 m^3 and because it is assumed to be independent of the depth of burial, the volume of the upper damage zone is obtained by subtracting the volume of the lower zone from the total. With a small depth of charge, the actual contribution of the upper damage zone to the total volume is quite small. As the depth of burial increases, the energy wasted in excessive breakage is gradually reduced and the volume in the upper damage zone increases, resulting in an increase of the total volume. In the numerical example, the volume of the upper damage zone reaches its maximum of 4.62 m^3 at a depth of charge slightly smaller than 1.2 m. Apparently, at the optimum point, the energy wasted in excessive breakage is minimum and the total energy utilization in rock fragmentation is maximum. The optimum point is the depth at which the two damage zones are completely coalesced without overlapping, yielding the maximum volume of fragments. However, the optimum depth of burial is also the starting point at which the two damage zones begin to separate if the depth of burial increases.

As the depth of burial further increases beyond the optimum, the upper damage zone tends to separate from the early formed lower damage zone. Due to the increase in the travel distance of the pressurized ring, a portion of the energy is dissipated in the rock mass before it reaches the ground surface. As a result, the volume of fragments in the upper damage zone decreases rapidly with the increase in the depth of burial.

The simulation results as demonstrated here tend to agree with the experimental findings by Livingston (Lang et al., 1977), who obtained the scaled volume versus scaled depth of burial relationship by a series of cratering tests. It has been found that the reason for the sudden drop in volume at charge depths larger than the optimum point is that the two damage zones begin to separate. As a result of the dissipation of the energy contained in the pressurized ring during its travel to the ground surface, the two damage zones are separated by an area that has very low damage value. With the increase in the depth of charge, this area expands and the upper damage zone recedes toward the borehole collar, diminishing in radius and depth below the ground surface. Figure 11 shows the reduced upper damage zone which is totally isolated from the lower damage zone at a depth of charge of 2.56 m. At a certain depth, the dissipation of the energy in the pressurized ring is so serious that there are no more fragments in the upper damage zone except for a few visible cracks radiating from the borehole mouth. When the visible cracks vanish at a even larger depth of burial, the upper damage zone has completely disappeared.

In addition to the total volume of material fragmented, fragment size distribution is another good measure of energy utilization during the process of rock fragmentation. Figure 12 shows a group of statistical fragment size distribution curves at different depths of charge. At a depth of burial of 0.96 m, the average fragment size is 135 mm, compared to the average fragment size of 141 mm (not shown in this figure) at the optimum depth of burial. As the depth of burial increases from 1.36 m to 2.0 m, the average fragment size increases steadily from 165 mm to 269 mm, and the size range of the fragments gets wider, i.e., the uniformity of fragment size distribution deteriorates.

Discussions on the Pressurized Ring

The pressurized ring is a new and useful concept introduced by the present work in describing stress wave propagation and rock mass response. The rock failure processes involved in a crater blasting can be explained by the formation and propagation of the pressurized ring generated by the explosive charge.

The pressurized ring is, in reality, a layer of rock material that is being compressed by the pressure front. Its shape in space before any reflection takes place is a hollow sphere, or ellipsoid, depending on the shape of the explosive charge and the point of initiation. The thickness of the pressurized ring is a very important parameter. Some important characteristics of the loading wave, such as the duration or frequency, is manifested by the pressurized ring. If the peak pressure is known, the loading rate as well as wave frequency can also be calculated using the thickness and the dilatation wave velocity.

The duration of the loading wave is one of the critical factors in the fracture process. Obviously, the thicker the pressurized ring, the longer the duration of the loading wave and the lower the wave frequency. Therefore, more energy is available for fueling the fracture process. It is known that given the same peak value, low frequency waves decay more slowly than high frequency ones and they do more damage to the rock mass or structures than the latter. Also, longer loading duration is associated with lower loading rates. Because the dynamic tensile strength for rock materials is approximately cube root dependent on the loading rate, a thicker pressurized ring would also mean lower loading rate and lower fracture stress in the failure process of a rock material, and eventually, better use of explosive energy for breaking the rock material.

As stated above, there are definite advantages to generating a pressurized ring as thick as possible for effective breakage of the rock material. Obviously, the thickness of the pressurized ring can be increased by using larger explosive charges. Therefore, for economical considerations, the thickness of the pressurized ring generated by the explosive charge should reasonably match the rock burden to be fractured. In cratering studies, it is also found that by shifting the initiation point of a given explosive charge, non-uniform pressurized rings can be achieved, significantly influencing the final blasting results. For example, when the explosive charge having a length/diameter ratio larger than a certain value is bottom initiated, a pressurized ring thicker in the upper part (which propagates toward the ground surface) and thinner in the bottom part is obtained, resulting in a larger volume of material fragmented and better fragmentation (Liu, 1996).

Conclusions

A number of conclusions can be drawn from this study under the simulation conditions:

1. Immediately after the detonation of the explosive charge, a thin layer of rock material confining the explosive charge fails under very high pressure and forms a crushed zone. The high pressure is mainly balanced by the plastic strain in this zone but it has negligible contribution to the total volume of fragments.
2. The rock mass outside the crushed zone is, at first elastically compressed, forming a pressurized ring prior to any kind of material failure. The characteristics of the ring such as its duration, frequency, and loading rate of the compressional wave are important for the development of damage and fragmentation that follow.
3. In crater blasting, there are two damage zones that are formed by different mechanisms. The lower damage zone is formed by tensile failure induced by the two tensile stress components that are developed in response to the action of the radial compressive stress in the pressurized ring; the upper damage zone is formed by the reflection of the pressurized ring from the ground surface. The formation of the upper damage zone is strongly influenced by the depth of burial of the explosive charge, but the lower damage zone is independent of the depth of burial.
4. The relationship between the two damage zones is determined by the depth of burial of the explosive charge. When the depth of burial is smaller than the optimum, two damage zones coalesce into one, forming a crater that can be excavated. When the depth of burial is larger than the optimum, the two damage zones begin to separate from each other. As the depth increases, the upper damage zone diminishes and finally disappears, and the lower damage zone cannot be excavated.
5. The average fragment size increases and the uniformity decreases with the increase in the depth of burial.

References

BAUER, A., HARRIES, G., LANG, R., PREZIOS, L., and SELLECK, D.J., 1965. How IOC puts crater research to work. Eng. Min. J., Vol. 166, No. 9, p.117-121.

BAWDEN, W.F., KATSABANIS, P.D., and YANG, R.L., 1993. Blast damage study by measurement and numerical modelling of blast damage and vibration in the area adjacent to the borehole, innovative mine design for the 21st century. Proceedings of the International Congress on Mine Design, Kingston, Ontario, Canada, August 23-26. p. 853-861.

BRINKMAN, J.R., 1987. Separating shock wave and gas expansion breakage mechanisms. Second International Symposium on Rock Fragmentation by Blasting, Keystone, Colorado, August 23 -26. p. 6-15.

COMEAU, W., 1995. Rock fragmentation by explosives — Myths and realities. Sixth High-Tech Seminar State-of-the-Art, Blasting Technology, Instrumentation and Explosive Applications, Boston, Massachusetts, United States, July 8-14.

DUVALL, W.I. and ATCHISON, T.C., 1957. Rock breakage by explosives. U.S. Bureau of Mines, Report of Investigations, No. 5356.

HAKALEHTO, K.O., 1969. The behavior of rocks under impulse loads. A study using the Hopkinson Split Bar Method. Doctoral Thesis, Technical University, Otoniemi-Helsinki. Acta Polytechnica Scadinavica, No. 81.

HIBBITT, KARLSSON & SORENSEN, INC., 1994a. ABAQUS/Explicit (version 5.4), User's Manual.

HIBBITT, KARLSSON & SORENSEN, INC., 1994b. An Introduction to ABAQUS/Explicit.

HOMMERT, P.J., KUSZMAUL, J.S., and PARRISH, R.L., 1987. Computational and experimental studies of the role of stemming in cratering. Second International Symposium on Rock Fragmentation by Blasting, Keystone, Colorado, August 23–27. p. 550-562.

KATSABANIS, P.D., 1994. Development of a model to predict the effects of delay blasting on rock fragmentation and throw, Phase I: Progress Report. Prepared for Thiokol Corporation, Elkton, Maryland, September 3.

KUTTER, H.K. and FAIRHURST, C., 1971. On the fracture process in blasting. Int. J. Rock Mech. Min. Sci., Vol. 8, p. 181-202.

LANG, L.C., 1976. The application of spherical charge technology in stope and pillar mining. E/MJ, May.

LANG, L.C., ROACH, R.J., and OSOKO, M.N., 1977. Spherical charge basis of VCR method. Canadian Mining Journal, September.

LeBLANC, T.M., HEILIG, J.H., and RYAN, J.M., 1995. Predicting the envelope of damage from the detonation of a confined charge. Sixth High-Tech Seminar State-of-the-Art, Blasting Technology, Instrumentation and Explosive Applications, Boston, Massachusetts, United States. July 8-14.

LIU, L., 1996. Continuum modelling of rock fragmentation by blasting. Ph.D Thesis, Department of Mining Engineering, Queen's University, Kinston, Ontario, December.

LIU, L. and KATSABANIS, P.D., 1997. Development of a continuum damage model for blasting analysis. Int. J. of Rock Mech. Sci. and Geomech. Abstr., Vol. 34, No. 2, p. 217-231. February.

LIVINGSTON, C.W., 1962. A Blasting Theory and Its Application, PR(R).

ROCQUE, P., 1992. Techniques utilized for the detection and characterization of blast induced damage. M.Sc. Eng. Thesis, Queen's University, Kingston, Ontario, Canada.

SIMHA, K.R.Y., FOURNEY, W.L., and DICK, R.D., 1987. An investigation of the usefulness of stemming in crater blasting. Second International Symposium on Rock Fragmentation by Blasting, Keystone, Colorado, August 23–27, p. 591-599.

WILSON, W.H., 1987. An experimental and theoretical analysis of stress wave and gas pressure effects in bench-blasting. Ph.D. Dissertation, University of Maryland.

ZHAO, Y., HUANG, J., and WANG, R., 1993. Fractal characteristics of mesofractures in compressed rock specimens. Int. J. Rock Mech. Min. Sci. & Geomech. Abstr., Vol. 30, No. 7, p. 877-882.